Electronic Supplementary Information

for

Electrophilicity of neutral square-planar organosilver(III) compounds

Daniel Joven-Sancho, Luca Demonti, Antonio Martín, Nathalie Saffon-Merceron,

Noel Nebra,* Miguel Baya, and Babil Menjón*

1. Experimental Section

General Procedures and Materials. Unless otherwise indicated, the reactions and manipulations were carried out under purified argon and exclusion of light using Schlenk techniques. Previously degassed solvents were dried using an MBraun SPS-800 System (CH_2Cl_2, *n*-hexane) or over activated 3 Å molecular sieves (Me_2CO, MeCN). The precursor material $[PPh_4][(CF_3)_3AgCl]$ was prepared using published methods.[S1] All other reagents were purchased from standard commercial suppliers and used as received. Elemental analyses were carried out using a Perkin Elmer 2400 CHNS/O Series II microanalyzer. IR spectra were recorded on neat solid samples using a PerkinElmer Spectrum FT-IR spectrometer ($4000–450$ cm^{-1}) equipped with an ATR device. NMR spectra were recorded at room temperature on Bruker ARX-300 or ARX-400 spectrometers. Chemical shifts of the measured nuclei (δ in ppm) are given with respect to the standard references in use: $SiMe_4$ (^1H), $CFCl_3$ (^{19}F) and 85% aq. H_3PO_4 (^{31}P). Multiplicity of the observed signals is indicated as follows: s = singlet, d = doublet, q = quartet, spt = septet, m = multiplet. Chemically inequivalent CF_3 groups are indicated as follows: CF_3–Ag–CF_3 refers to the mutually *trans*-standing CF_3 groups (q), whereas CF_3–Ag–L refers to the CF_3 group *trans* to the neutral L ligand (spt).

CAUTION: Thallium compounds are highly toxic and must be handled with special care.

Synthesis of $(CF_3)_3Ag(NCMe)$ (1): $TlClO_4$ (97.8 mg, 0.322 mmol) was added to a solution of $[PPh_4][(CF_3)_3AgCl]$ (200 mg, 0.28 mmol) in 5 cm^3 of MeCN at 233 K. After 15 min of stirring, the suspension was concentrated to *ca*. 0.5 cm^3 and the resulting residue was extracted with Et_2O (8×3 cm^3) at 195 K. The extract was filtered and the filtrate was evaporated to dryness. By treatment of the resulting residue with *n*-hexane (3×2 cm^3) at 195 K, a white solid was obtained, which was identified as compound **1** (25 mg, 0.07 mmol, 25% yield). The compound decomposes readily in the solid state on standing, being unstable even at 243 K. In contrast, MeCN solutions are significantly more stable: they can be stored for months at 243 K without significant decomposition and are therefore preferred for synthetic use. **^{19}F NMR** (282.231 MHz, CD_3CN, 298 K;

Fig. S1): δ_F /ppm = −22.73 [two (52:48) dspt, 3F, $^2J(^{109}\text{Ag,F}) = 91.5$ Hz, $^4J(\text{F, F}) = 9.5$ Hz; CF$_3$–Ag–L], −32.67 ppm [two (52:48) dq, 6F, $^2J(^{109}\text{Ag,F}) = 22.7$ Hz; CF$_3$–Ag–CF$_3$]. No satisfactory elemental analyses were obtained owing to the instability of the substance and the ease with which it releases MeCN. **Single crystals** suitable for X-ray diffraction were obtained by slow diffusion at 4 °C of a layer of *n*-hexane (3 cm^3) into a solution of compound **1** in Et$_2$O/MeCN (150 mm^3; 95/5) at −30 °C.

Synthesis of (CF$_3$)$_3$Ag(py) (2): To a solution of compound **1** (50 mg, 0.14 mmol) in 2 cm^3 of MeCN, previously dried and degassed py (22.7 mm^3, 0.28 mmol) was added and the solution was stirred at room temperature for 5 min. After removal of the solvent in vacuo for 4 h, a white solid was obtained, which was identified as compound **2** (48 mg, 0.141 mmol, 86% yield). **^{1}H NMR** (300 MHz, CD$_2$Cl$_2$, 298 K): δ_H /ppm = 8.59 [dt, 2H, $^2J(\text{H,H}) = 4.92$ Hz, $^3J(\text{H,H}) = 1.53$ Hz; *ortho*-H], 8.13 [tt, 1H, $^2J(\text{H,H}) = 7.76$ Hz, $^3J(\text{H,H}) = 1.53$ Hz; *para*-H], 7.71 (m, 2H; *meta*-H). **^{19}F NMR** (376.49 MHz, CD$_2$Cl$_2$, 298 K; Fig. S2): δ_F /ppm = −22.33 [two (52:48) dspt, 3F, $^2J(^{109}\text{Ag,F}) = 75.8$ Hz, $^4J(\text{F,F}) = 9.3$ Hz; CF$_3$–Ag–L], −34.14 [two (52:48) dq, 6F, $^2J(^{109}\text{Ag,F}) = 29.0$ Hz; CF$_3$–Ag–CF$_3$]. **Elemental analysis** (%) calcd for C$_8$H$_5$AgF$_9$N: C 24.4, H 1.3, N: 3.6; found, C: 24.3, H: 1.3, N: 3.7. **Single crystals** suitable for X-ray diffraction purposes were obtained by slow diffusion of *n*-pentane (3 cm^3) into a solution of compound **2** in CH$_2$Cl$_2$ (150 mm^3) at −30 °C. **Single crystals** or the solvates **2**·NCMe and **2**·py suitable for X-ray diffraction purposes were respectively obtained in the presence of either NCMe or py.

Synthesis of (CF$_3$)$_3$Ag(dmap) (3): To a solution of compound **1** (100 mg, 0.28 mmol) in 3 cm^3 of MeCN, 4-dimethylaminopyridine (34.20 mg, 0.28 mmol) was added and the solution was stirred at room temperature for 5 min. After removing the solvent in vacuo and treating the residue with cold *n*-hexane (2 × 1 cm^3), a white solid was obtained, which was identified as compound **3** (69 mg, 0.098 mmol, 35% yield). **IR** (ATR): $\tilde{v}$ /cm^{-1} = 2936 (w), 1620 (s), 1543 (m), 1394 (m), 1235 (w), 1128 (m), 1059 (vs), 999 (vs), 948 (m), 809 (vs), 724 (s), 709 (m), 524 (m), 311 (s). **^{1}H NMR** (300 MHz, CD$_2$Cl$_2$,

298 K): δ_H /ppm = 7.98 (br s, 2H; *ortho*-H), 6.68 (br s, 2H; *meta*-H), 3.13 (s, 6H; Me). **^{19}F NMR** (282.231 MHz, CD$_2$Cl$_2$, 298 K; Fig. S3): δ_F /ppm = −23.73 [two (52:48) dspt, 3F, $^2J(^{109}Ag,F)$ = 70.4 Hz, $^4J(F,F)$ = 9.0 Hz; CF$_3$–Ag–L], −34.34 [two (52:48) dq, 6F, $^2J(^{109}Ag,F)$ = 30.7 Hz, $^4J(F,F)$ = 9.0Hz; CF$_3$–Ag–CF$_3$]. **Elemental analysis** (%) calcd for C$_{10}$H$_{10}$AgF$_9$N$_2$: C 27.5, H 2.3, N 6.4; found: C 27.7, H 2.4, N 6.4. **Single crystals** suitable for X-ray diffraction purposes were obtained by slow diffusion of a *n*-hexane (3 cm^3) layer into a solution of 10 mg of compound **3** in CH$_2$Cl$_2$ (150 mm^3) at −30 °C.

Synthesis of (CF$_3$)$_3$Ag(PPh$_3$) (4): To a solution of compound **1** (100 mg, 0.28 mmol) in 3 cm^3 of MeCN, PPh$_3$ (50.45 mg, 0.28 mmol) was added and the solution was stirred at room temperature for 5 min. After removing the solvent in vacuo and treating the residue with cold *n*-hexane (2 × 1 cm^3), a white solid was obtained, which was identified as compound **4** (49 mg, 0.10 mmol, 36% yield). **IR** (ATR): $\tilde{v}$ /cm^{-1} = 3062 (w), 2963 (w), 2255 (w), 1483 (w), 1438 (m), 1109 (s), 1044 (vs), 993 (vs), 745 (vs), 709 (m), 670 (vs), 520 (s), 508 (s), 494 (s), 449 (m), 428 (w), 291 (vs). **^{1}H NMR** (300 MHz, CD$_2$Cl$_2$, 193 K): δ_H /ppm = 7.68–7.61 (m, 9H; aromatics), 7.54 (m, 6H; aromatics). **^{19}F NMR** (282.231 MHz, CD$_2$Cl$_2$, 193 K; Fig. S4): δ_F /ppm = −27.12 [two (52:48) not well-resolved dspt, 3F, $^2J(P,F)$ = 159.28 Hz, $^2J(^{109}Ag,F)$ = 60.93 Hz; CF$_3$–Ag–L], −28.08 [two (52:48) dq, 6F, $^2J(^{109}Ag,F)$ = 41.30 Hz; CF$_3$–Ag–CF$_3$] (simulated in Fig. S6a). **^{31}P NMR** (121.442 MHz, CD$_2$Cl$_2$, 193 K; Fig. S5): δ_P /ppm = 28.84 ppm (simulated in Fig. S6b). **Elemental analysis** (%) C$_{21}$H$_{15}$AgF$_9$P: C 43.7, H 2.6; found: C 43.1, H 2.6. **Single crystals** suitable for X-ray diffraction purposes were obtained by slow diffusion of a *n*-hexane (3 cm^3) layer into a solution of 10 mg of compound **4** in CH$_2$Cl$_2$ (150 mm^3) at −30 °C.

Synthesis of (CF$_3$)$_3$Ag(AsPh$_3$) (5): To a solution of compound **1** (100 mg, 0.28 mmol) in 3 cm^3 of CH$_2$Cl$_2$, AsPh$_3$ (85.74 mg, 0.28 mmol) was added and the solution was stirred at room temperature for 5 min. After removing the solvent in vacuo and treating the residue with cold *n*-hexane (2 × 1 cm^3), a pale-yellow solid was obtained,

which was identified as compound **5** (46 mg, 0.078 mmol, 28% yield). **IR** (ATR): $\tilde{v}$ /cm^{-1} = 3058 (w), 1650 (w), 1578 (w), 1484 (m), 1438 (m), 1120 (s), 1052 (vs), 1029 (vs) 993 (vs), 739 (s), 731 (s), 716 (m), 688 (m), 527 (w), 517 (w), 480 (s), 466 (s), 347 (m), 333 (m), 325 (s), 317 (s). **^{19}F NMR** (282.231 MHz, CD$_2$Cl$_2$, 193 K; Fig. S7): δ_F /ppm = -24.40 (dm, 3F, $^2J(^{109}Ag,F)$ unresolved; CF$_3$–Ag–L), -25.52 (m, 6F, $^2J(^{109}Ag,F)$ unresolved; CF$_3$–Ag–CF$_3$). **Elemental analysis** (%) C$_{21}$H$_{15}$AgF$_9$As: C 40.6, H 2.4; found: C 40.7, H 2.5. **Single crystals** suitable for X-ray diffraction purposes were obtained by slow diffusion of a *n*-hexane (3 cm^3) layer into a solution of 10 mg of compound **5** in 10:1 Et$_2$O/Me$_2$CO (150 mm^3) at -30 °C.

Table S1. ^{19}F NMR spectroscopic parameters independently assigned by Naumann[a] and Eujen[b] to the (CF$_3$)$_3$AgNCMe complex in MeCN solution.
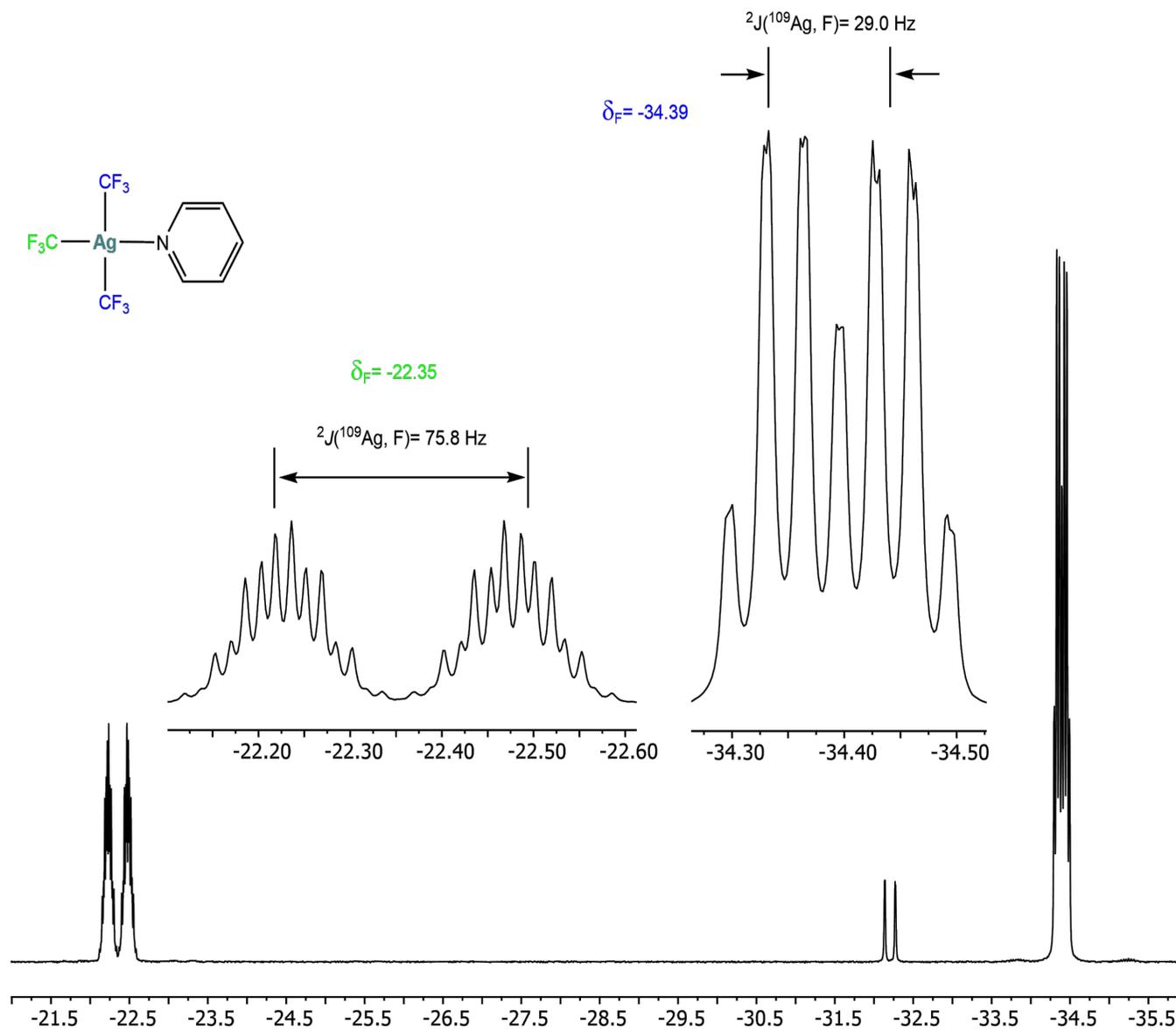
δ_F /ppm	$^2J(^{109}Ag,^{19}F)$ /Hz	$^4J(^{19}F,^{19}F)$ /Hz
-21.7 (spt) / -21.5	91.2 / 85.3	9.5 /
-31.6 (q) / -36.4	22.6 / 25.5	9.0 (*cis*) & 19 (*trans*)

[a] See Ref. S2 (*T* = 20 °C). [b] See Ref. S3 (*T* = -25 °C).
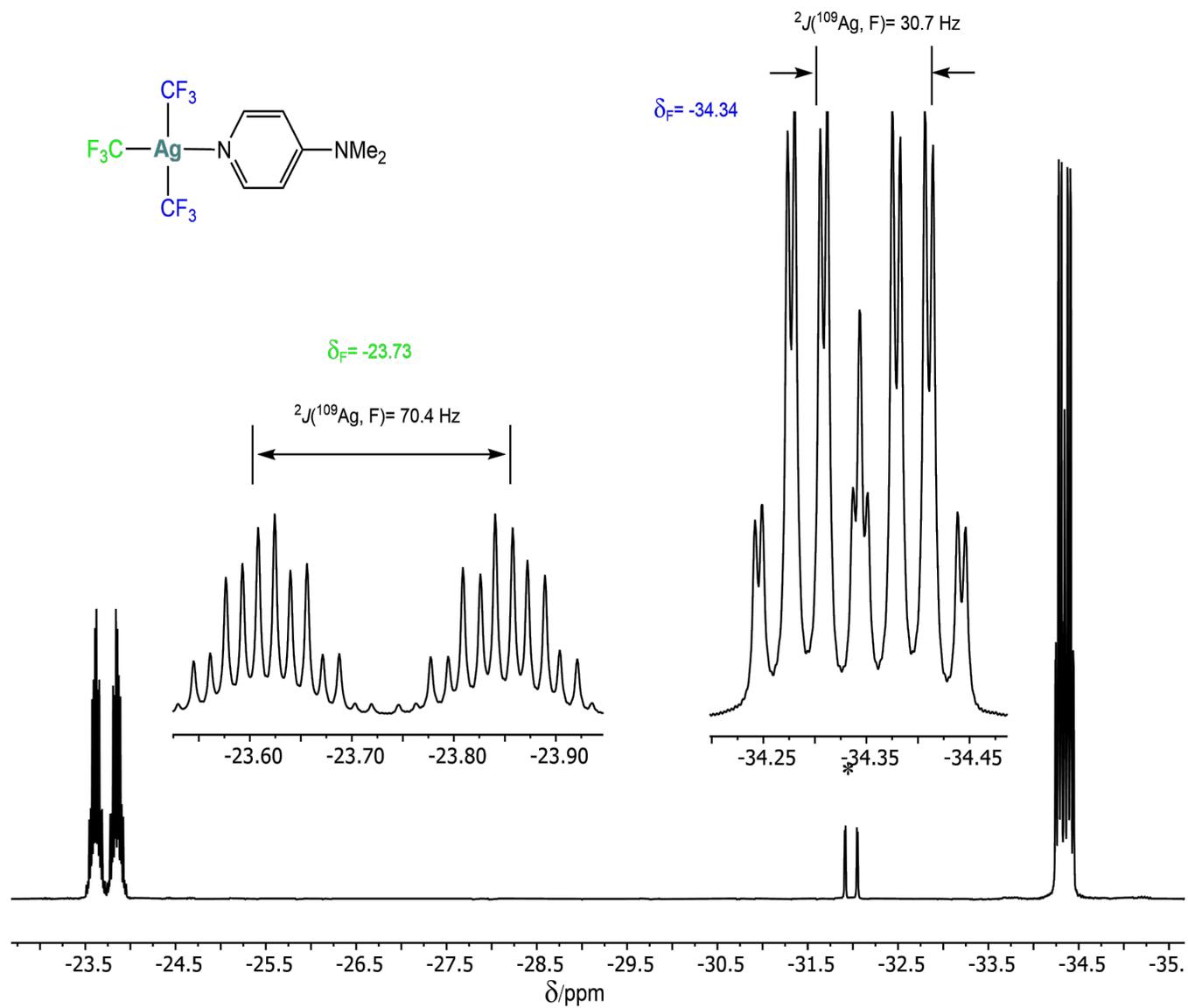
2. NMR Spectra
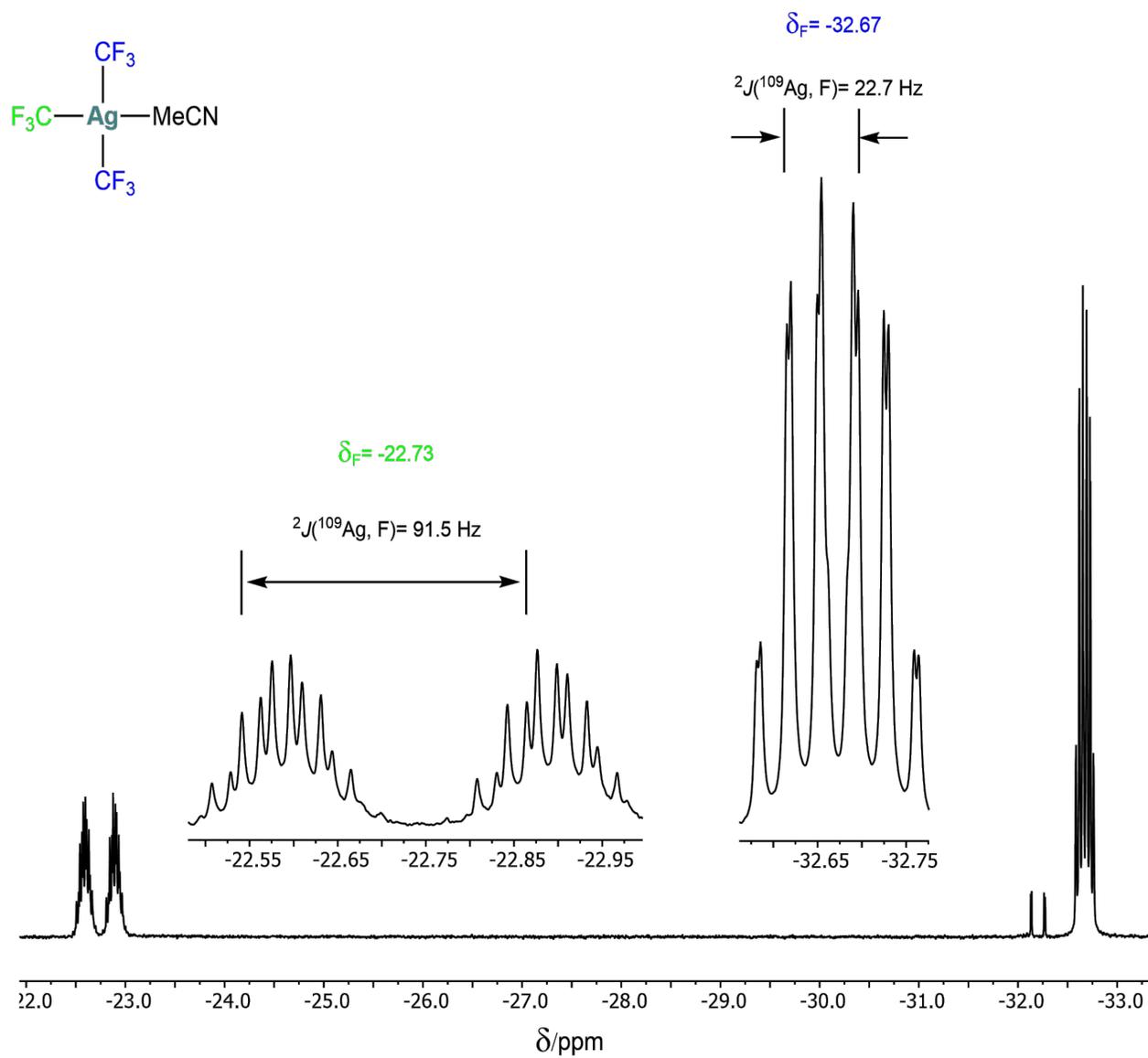
Fig. S1. ^{19}F NMR spectrum (282.231 MHz, CD$_3$CN, 298 K) of (CF$_3$)$_3$Ag(NCMe)] (**1**).

Fig. S2. ^{19}F NMR spectrum (376.49 MHz, CD$_2$Cl$_2$, 298 K) of (CF$_3$)$_3$Ag(py) (**2**).

Fig. S3. ^{19}F NMR spectrum (282.231 MHz, CD$_2$Cl$_2$, 298 K) of (CF$_3$)$_3$Ag(dmap) (**3**).
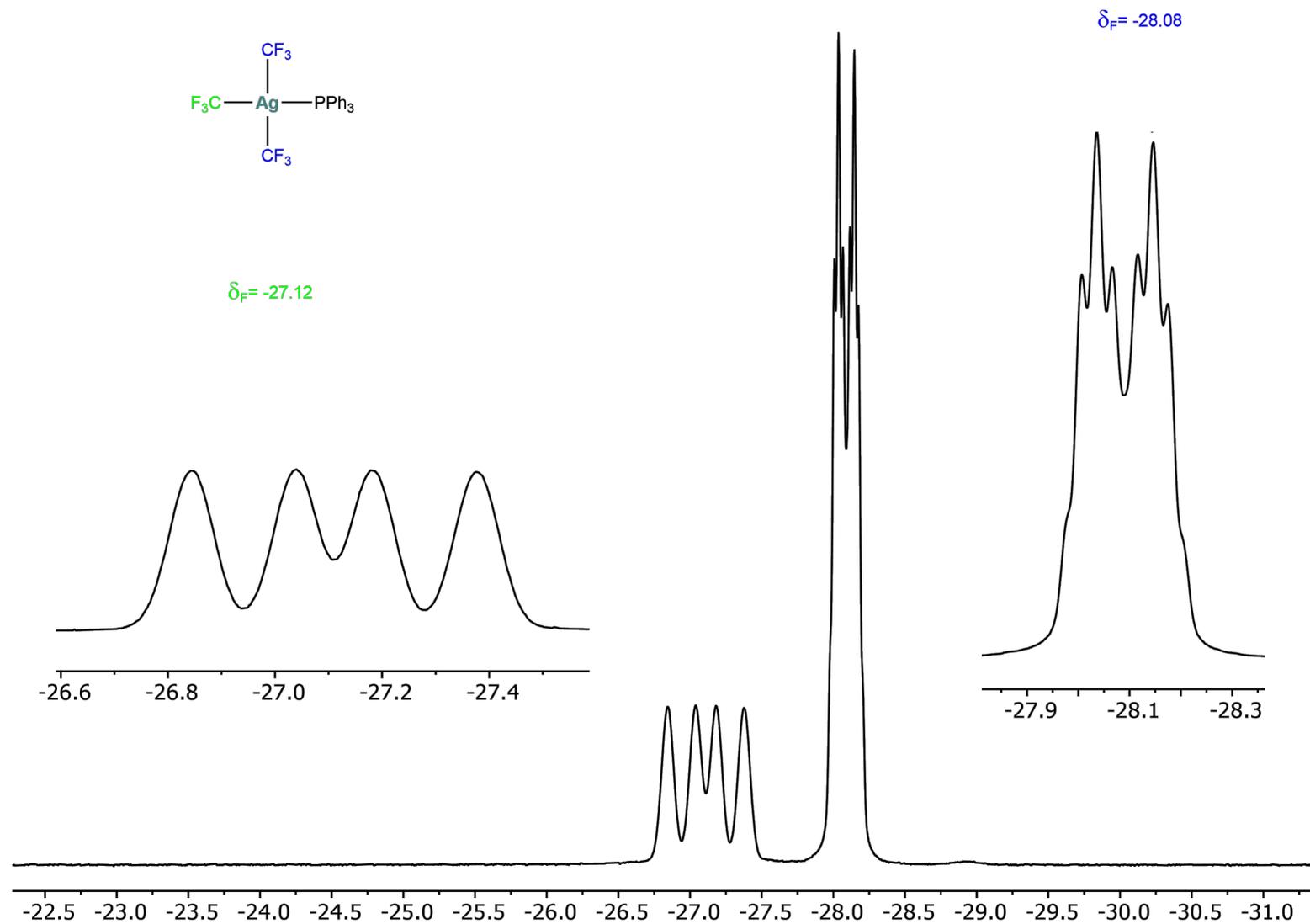
Fig. S4. ^{19}F NMR spectrum (282.231 MHz, CD$_2$Cl$_2$, 298 K) of (CF$_3$)$_3$Ag(PPh$_3$) (**4**). The spectrum is simulated in Fig. S6a.

a)
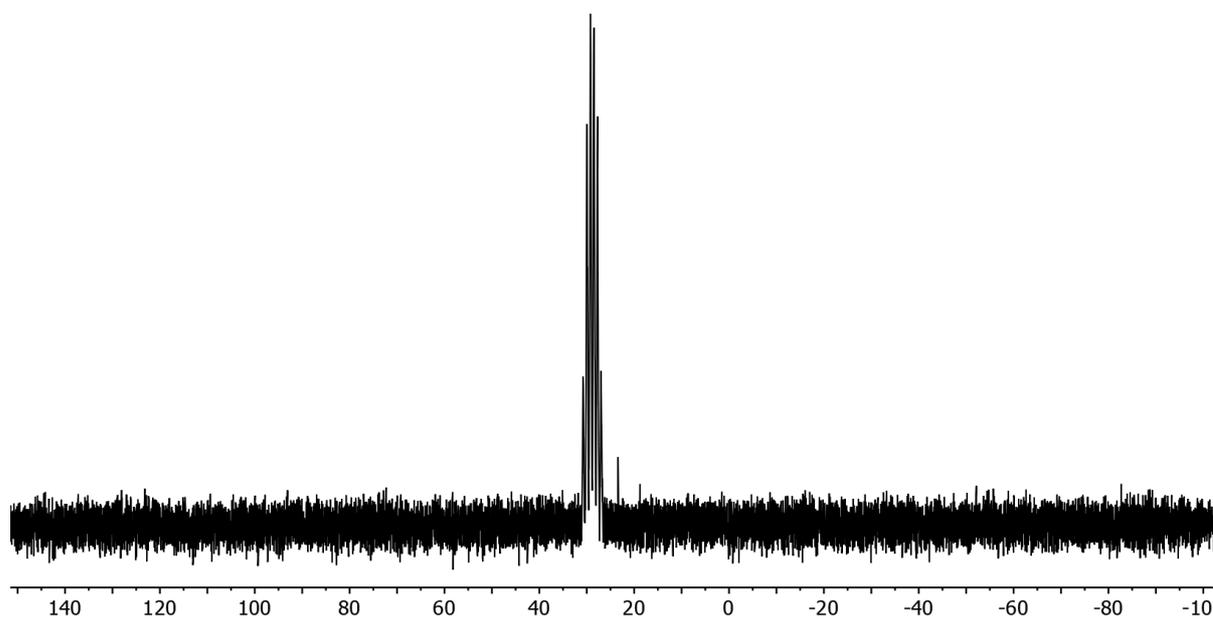
b)
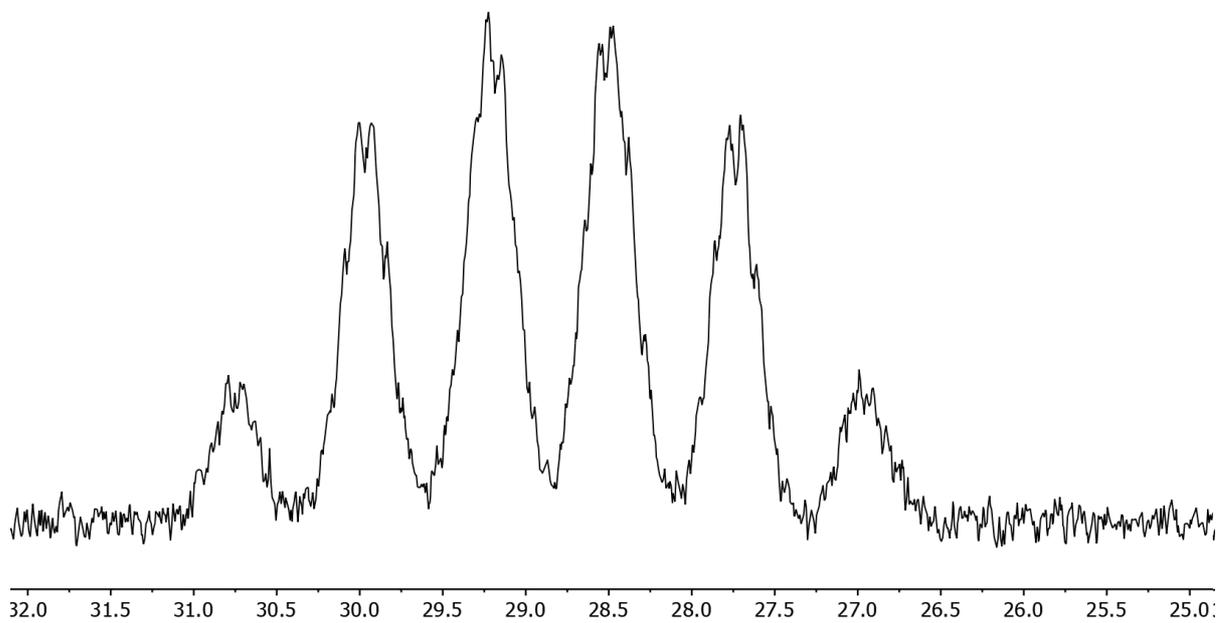
Fig. S5. ^{31}P NMR spectrum (121.442 MHz, CD$_2$Cl$_2$, 298 K) of (CF$_3$)$_3$Ag(PPh$_3$) (**4**): a) overall view; b) detail of the characteristic signal. The spectrum is simulated in Fig. S6b.

	^{31}P		
^{19}F (CF$_3$-Ag-P)	94.0	^{19}F (CF$_3$-Ag-P)	
^{19}F (CF$_3$-Ag-CF$_3$)	10.0	8.0	^{19}F (CF$_3$-Ag-CF$_3$)
^{109}Ag / ^{107}Ag	190.0 / 165.8	59.8 / 52.2	34.8 / 30.4
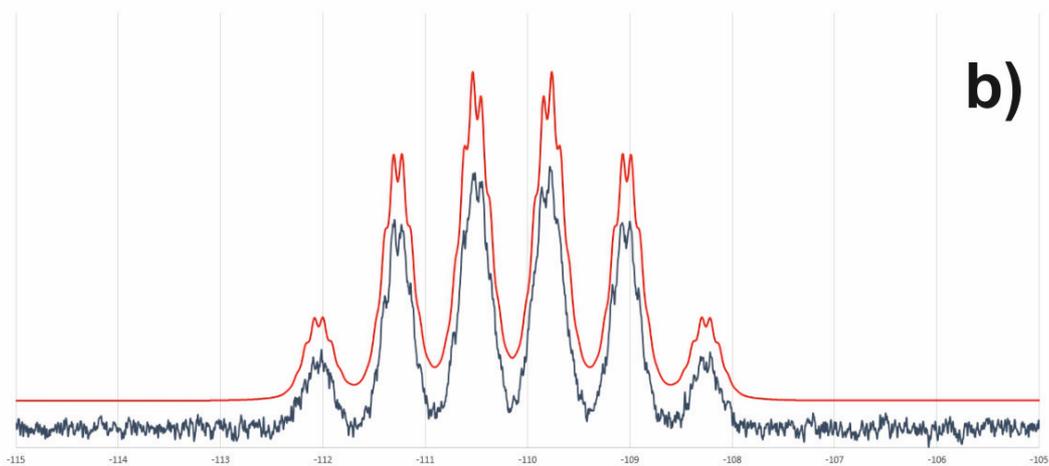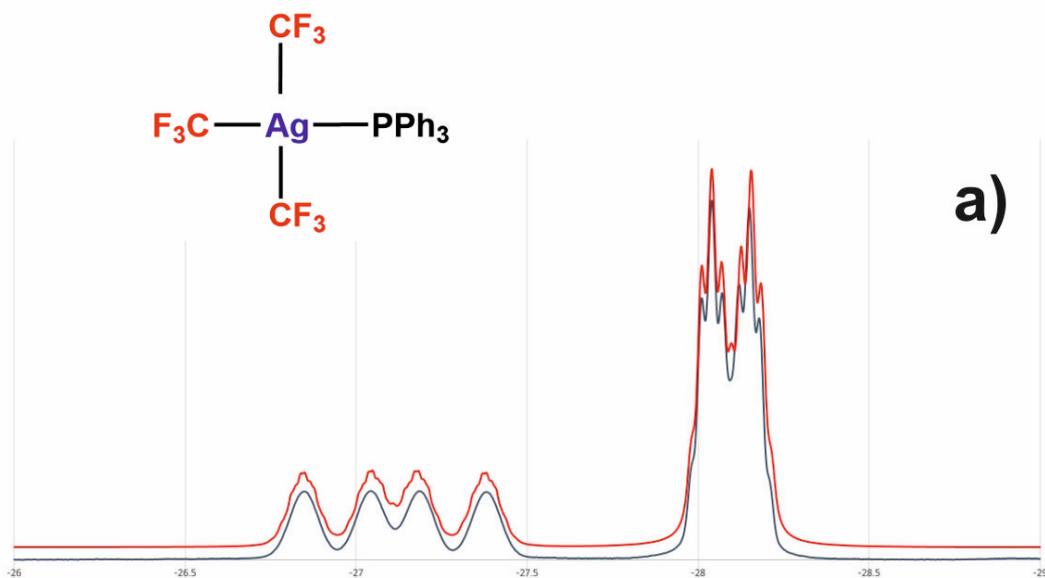
Fig. S6. Simulated (red) vs experimental (black) ^{19}F (a) and ^{31}P (b) NMR spectra of (CF$_3$)$_3$Ag(PPh$_3$) (**4**) using the set of parameters given above.
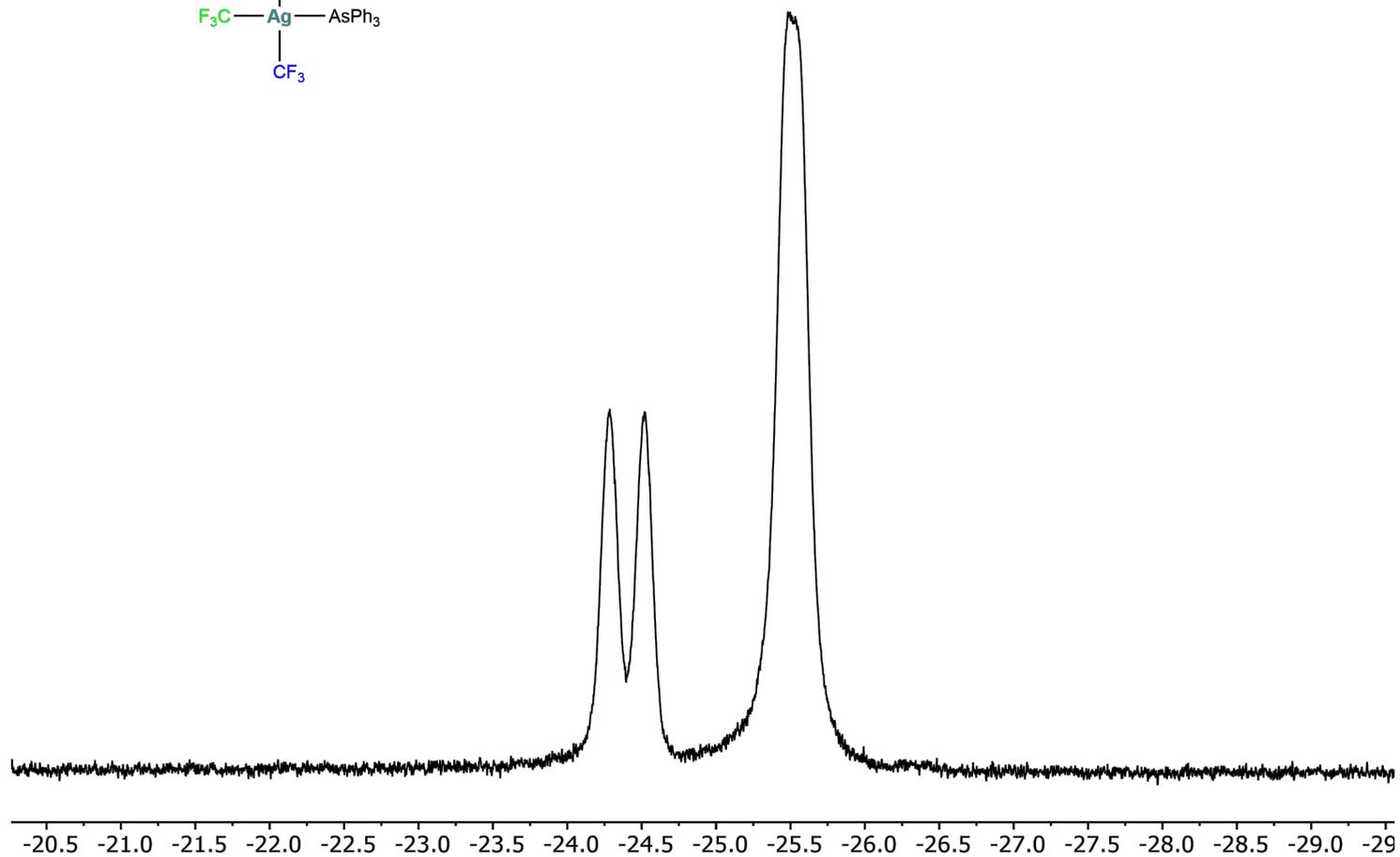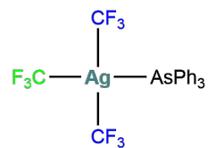
Fig. S7. ^{19}F NMR spectrum (282.231 MHz, CD$_2$Cl$_2$, 298 K) of (CF$_3$)$_3$Ag(AsPh$_3$) (**5**).

3. Crystal Data and Structure Refinement

Crystal data and other details of the structure analysis are presented in Tables S2, S4, S6, S8, S10, S12, S14. Single crystals suitable for X-ray diffraction studies were obtained as indicated in the corresponding Experimental entry. Crystals were mounted at the end of quartz fibres. The radiation used in all cases was graphite-monochromated Mo-Kα (λ = 71.073 pm). X-ray intensity data were collected on an Oxford Diffraction Xcalibur (**1**, **3**, **4**·¼CH$_2$Cl$_2$ and **5**·Me$_2$CO) or a Bruker D8 VENTURE Photon III-C14 (**2**, **2**·NCMe and **2**·py) diffractometer. Data collection was performed at the temperature indicated in each entry. The diffraction frames were integrated and corrected from absorption by using the CrysAlis Pro program[S4] (**1**, **3**, **4**·¼CH$_2$Cl$_2$ and **5**·Me$_2$CO) or by using the SADABS software[S5] (**2**, **2**·NCMe and **2**·py).

The structures were solved by Patterson and Fourier methods and refined by full-matrix least squares on F^2 with SHELXL.[S6] All non-H atoms were assigned anisotropic displacement parameters and refined without positional constraints. The positions of the H atoms were constrained to idealised geometries and assigned isotropic displacement parameters equal to 1.2 times the U_{iso} values of their respective parent atoms. For **2**, all the CF$_3$ groups were rotationally disordered and each of the corresponding F atoms was refined over two positions with unequal partial occupancy. For **4**·¼CH$_2$Cl$_2$, a CH$_2$Cl$_2$ solvent moiety is disordered over two positions near an inversion centre which were refined with 0.3/0.2 partial occupancy. Restrains were used in its geometry as well as in some of the anistrotropic thermal parameters of its atoms.

Full-matrix least-squares refinement of these models against F^2 converged to final residual indices given in Tables S2, S4, S6, S8, S10, S12, S14. Selected interatomic distances and angles are given in Tables S3, S5, S7, S9, S11, S13, S15.

Table S2. Crystal data and structure refinement for compound (CF$_3$)$_3$Ag(NCMe) (**1**)

formula	C$_5$H$_3$AgF$_9$N
M_t [g mol^{-1}]	355.95
T [K]	100(1)
λ [pm]	71.073
crystal system	monoclinic
space group	$P2_1/n$
a [pm]	792.74(2)
b [pm]	685.92(1)
c [pm]	1786.81(4)
β [°]	101.645(2)
V [nm^3]	0.95159(3)
Z	4
ρ [g cm^{-3}]	2.485
μ [mm^{-1}]	2.229
$F(000)$	672
2θ range [°]	6.4–56.6
no. of reflns colltd	17583
no. of unique reflns	2191
R_{int}	0.0240
R indices [$I > 2\sigma(I)$][a]	
R_1	0.0175
wR_2	0.0430
R indices (all data)	
R_1	0.0182
wR_2	0.0433
goodness-of-fit[b] on F^2	1.058
CCDC no.	2226904

[a] $R_1 = \Sigma(|F_o| - |F_c|) / \Sigma|F_o|$; $wR_2 = [\Sigma w(F_o^2 - F_c^2)^2 / \Sigma w(F_o^2)^2]^{1/2}$.

[b] Goodness-of-fit $= [\Sigma w(F_o^2 - F_c^2)^2 / (n_{obs} - n_{param})]^{1/2}$.
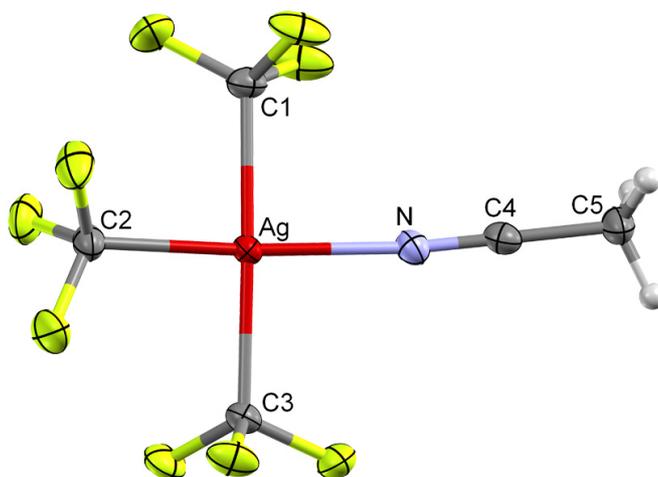
Table S3. Interatomic distances [pm] and angles [°] for $(CF_3)_3Ag(NCMe)$ as found in crystals of **1** with atom labelling as indicated above.

Ag–C(1)	211.08(19)	C(1)–Ag–C(2)	89.54(8)
Ag–C(2)	205.10(18)	C(1)–Ag–C(3)	174.27(7)
Ag–C(3)	210.46(18)	C(1)–Ag–N	87.72(7)
Ag–N	209.05(16)	C(2)–Ag–C(3)	90.53(7)
N–C(4)	113.2(2)	C(2)–Ag–N	174.12(7)
C(4)–C(5)	144.8(3)	C(3)–Ag–N	92.71(7)
av. C(1)–F	134.4(2)		
av. C(2)–F	133.3(2)	av. Ag–C(1)–F	104.93(17)
av. C(3)–F	135.1(2)	av. Ag–C(2)–F	106.84(16)
		av. Ag–C(3)–F	105.37(15)
Ag–N–C(4)	173.22(16)		
N–C(4)–C(5)	179.7(2)	av. F–C(1)–F	113.62(13)
		av. F–C(2)–F	111.98(13)
		av. F–C(3)–F	113.28(12)

Table S4. Crystal data and structure refinement for compound (CF$_3$)$_3$Ag(py) (**2**)

formula	C$_8$H$_5$AgF$_9$N
M_t [g mol^{-1}]	394.00
T [K]	193(2)
λ [pm]	71.073
crystal system	orthorhombic
space group	$P2_12_12_1$
a [pm]	749.04(3)
b [pm]	927.69(4)
c [pm]	1720.85(8)
V [nm^3]	1.19578(9)
Z	4
ρ [g cm^{-3}]	2.189
μ [mm^{-1}]	1.786
$F(000)$	752
2θ range [°]	5.0–56.6
no. of reflns colltd	36668
no. of unique reflns	2957
R_{int}	0.0370
R indices [$I > 2\sigma(I)$][a]	
R_1	0.0283
wR_2	0.0609
R indices (all data)	
R_1	0.0358
wR_2	0.0643
absolute structure factor	−0.023(13)
goodness-of-fit[b] on F^2	1.046
CCDC no.	2226905

[a] $R_1 = \Sigma(|F_o| - |F_c|) / \Sigma|F_o|$; $wR_2 = [\Sigma w(F_o^2 - F_c^2)^2 /\Sigma w(F_o^2)^2]^{1/2}$.
[b] Goodness-of-fit $= [\Sigma w(F_o^2 - F_c^2)^2 / (n_{obs} - n_{param})]^{1/2}$.

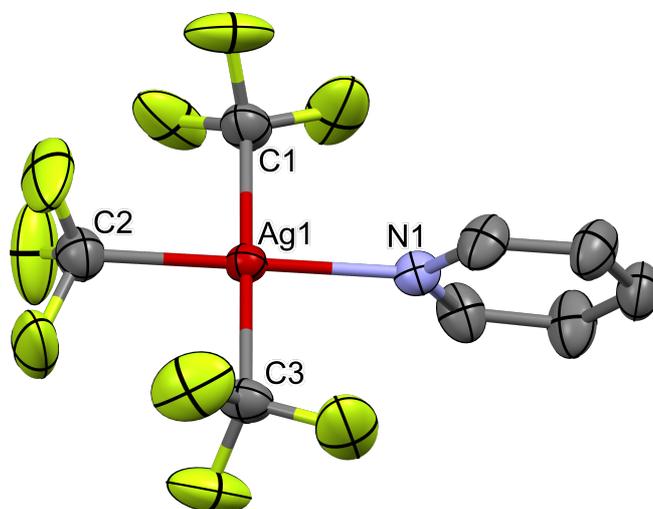**Table S5**. Interatomic distances [pm] and angles [°] for $(CF_3)_3Ag(py)$ as found in crystals of **2** with atom labelling as indicated above.[a]

Ag–C(1)	209.9(6)	C(1)–Ag–C(2)	89.8(2)
Ag–C(2)	205.1(6)	C(1)–Ag–C(3)	179.5(2)
Ag–C(3)	210.0(6)	C(1)–Ag–N	89.6(2)
Ag–N	211.4(4)	C(2)–Ag–C(3)	90.1(2)
av. C(1)–F	131.8(12)	C(2)–Ag–N	178.7(2)
av. C(2)–F	130.3(12)	C(3)–Ag–N	90.4(2)
av. C(3)–F	132.5(17)		
		av. Ag–C(1)–F	115.1(7)
		av. Ag–C(2)–F	113.7(7)
		av. Ag–C(3)–F	113.3(10)
		av. F–C(1)–F	103.2(11)
		av. F–C(2)–F	104.8(12)
		av. F–C(3)–F	105.2(14)

[a] Only one set of the rotationally disordered F atoms is shown in the image above.

Table S6. Crystal data and structure refinement for compound $(CF_3)_3Ag(py)\cdot NCMe$ (**2**$\cdot$NCMe)

formula	$C_{10}H_8AgF_9N_2$
M_t [g mol^{-1}]	435.05
T [K]	193(2)
λ [pm]	71.073
crystal system	triclinic
space group	$P\bar{1}$
a [pm]	818.28(7)
b [pm]	902.35(7)
c [pm]	1009.23(8)
α [°]	92.634(3)
β [°]	92.974(3)
γ [°]	106.819(3)°.
V [nm^3]	0.71090(10)
Z	2
ρ [g cm^{-3}]	2.032
μ [mm^{-1}]	1.514
$F(000)$	420
2θ range [°]	5.9–56.6
no. of reflns colltd	25335
no. of unique reflns	3528
R_{int}	0.0586
R indices [$I > 2\sigma(I)$][a]	
$\quad R_1$	0.0311
$\quad wR_2$	0.0626
R indices (all data)	
$\quad R_1$	0.0430
$\quad wR_2$	0.0667
goodness-of-fit[b] on F^2	1.074
CCDC no.	2226906

[a] $R_1 = \sum(|F_o| - |F_c|) / \sum|F_o|$; $wR_2 = [\sum w(F_o^2 - F_c^2)^2 / \sum w(F_o^2)^2]^{1/2}$.
[b] Goodness-of-fit $= [\sum w(F_o^2 - F_c^2)^2 / (n_{obs} - n_{param})]^{1/2}$.

Table S7. Interatomic distances [pm] and angles [°] for $(CF_3)_3Ag(py)\cdot NCMe$ as found in crystals of **2**·NCMe with atom labelling as indicated above.[a]

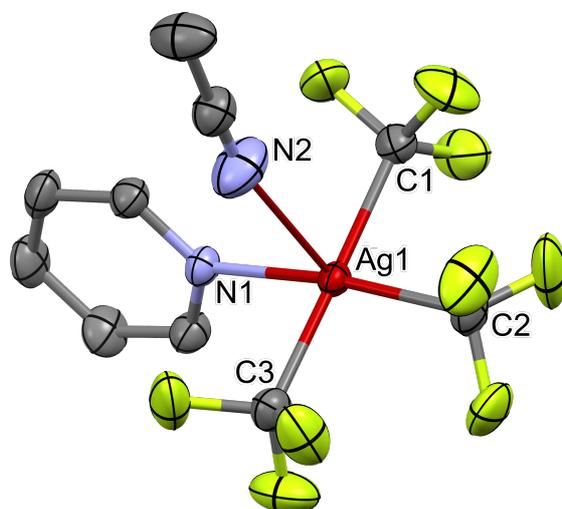|			
Ag–C(1)	210.8(3)	C(1)–Ag–C(2)	90.01(13)
Ag–C(2)	205.9(3)	C(1)–Ag–C(3)	176.86(14)
Ag–C(3)	209.6(3)	C(1)–Ag–N(1)	92.77(11)
Ag–N(1)	213.4(2)	C(2)–Ag–C(3)	89.32(13)
av. C(1)–F	134.5(4)	C(2)–Ag–N(1)	169.96(12)
av. C(2)–F	132.6(4)	C(3)–Ag–N(1)	88.41(11)
av. C(3)–F	134.4(4)		
		av. Ag–C(1)–F	113.7(2)
Ag···N(2)	278.4(3)	av. Ag–C(2)–F	112.7(2)
		av. Ag–C(3)–F	113.7(2)
		av. F–C(1)–F	104.9(3)
		av. F–C(2)–F	106.1(3)
		av. F–C(3)–F	104.9(3)

[a] The Ag–N(2) line deviates just 2.5(5)° from the normal to the best basal plane.

Table S8. Crystal data and structure refinement for compound $(CF_3)_3Ag(py)\cdot py$ (**2**·py)

formula	$C_{13}H_{10}AgF_9N_2$
M_t [g mol^{-1}]	473.10
T [K]	193(2)
λ [pm]	71.073
crystal system	orthorhombic
space group	*Pbca*
a [pm]	1412.38(16)
b [pm]	1258.90(15)
c [pm]	1809.4(2)
V [nm^3]	3.2171(7)
Z	8
ρ [g cm^{-3}]	1.954
μ [mm^{-1}]	1.347
$F(000)$	1840
2θ range [°]	6.6–48.8
no. of reflns colltd	62109
no. of unique reflns	2640
R_{int}	0.1784
R indices [$I > 2\sigma(I)$]^a	
R_1	0.0428
wR_2	0.0865
R indices (all data)	
R_1	0.0922
wR_2	0.1094
goodness-of-fit^b on F^2	1.045
CCDC no.	2226907

^{a} $R_1 = \Sigma(|F_o| - |F_c|) / \Sigma|F_o|$; $wR_2 = [\Sigma w(F_o^2 - F_c^2)^2 / \Sigma w(F_o^2)^2]^{1/2}$.
^{b} Goodness-of-fit $= [\Sigma w(F_o^2 - F_c^2)^2 / (n_{obs} - n_{param})]^{1/2}$.
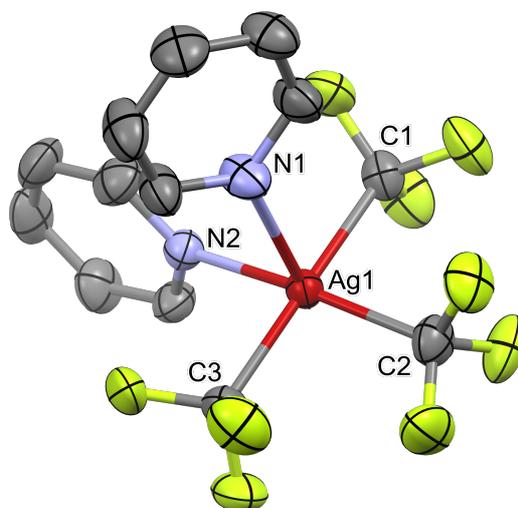
Table S9. Interatomic distances [pm] and angles [°] for $(CF_3)_3Ag(py)\cdot py$ as found in crystals of **2**·py with atom labelling as indicated above.[a]

Ag–C(1)	208.3(7)	C(1)–Ag–C(2)	89.1(3)
Ag–C(2)	205.2(7)	C(1)–Ag–C(3)	176.8(3)
Ag–C(3)	209.3(7)	C(1)–Ag–N(2)	87.7(2)
Ag–N(2)	213.1(5)	C(2)–Ag–C(3)	91.9(3)
		C(2)–Ag–N(2)	166.2(3)
av. C(1)–F	134.9(8)	C(3)–Ag–N(2)	90.5(2)
av. C(2)–F	133.9(8)		
av. C(3)–F	134.9(9)	av. Ag–C(1)–F	113.8(5)
		av. Ag–C(2)–F	113.1(5)
Ag···N(1)	263.6(5)	av. Ag–C(3)–F	114.1(5)
		av. F–C(1)–F	104.7(6)
		av. F–C(2)–F	105.6(6)
		av. F–C(3)–F	104.4(6)

[a] The Ag–N(1) line deviates just 1.8(5)° from the normal to the best basal plane.

Table S10. Crystal data and structure refinement for compound $(CF_3)_3Ag(dmap)$ (**3**)

formula	$C_{10}H_{10}AgF_9N_2$
M_t [g mol^{-1}]	437.07
T [K]	100(2)
λ [pm]	71.073
crystal system	monoclinic
space group	$P2_1/c$
a [pm]	500.405(14)
b [pm]	2213.54(6)
c [pm]	1240.17(4)
β [°]	93.858(3)
V [nm^3]	1.37059(7)
Z	4
ρ [g cm^{-3}]	2.118
μ [mm^{-1}]	1.571
$F(000)$	848
2θ range [°]	6.4–56.6
no. of reflns colltd	11462
no. of unique reflns	2955
R_{int}	0.0354
R indices $[I > 2\sigma(I)]^a$	
$\quad R_1$	0.0299
$\quad wR_2$	0.0588
R indices (all data)	
$\quad R_1$	0.0457
$\quad wR_2$	0.0632
goodness-of-fit^b on F^2	1.067
CCDC no.	2226908

[a] $R_1 = \Sigma(|F_o| - |F_c|) / \Sigma|F_o|$; $wR_2 = [\Sigma w(F_o^2 - F_c^2)^2 / \Sigma w(F_o^2)^2]^{1/2}$.
[b] Goodness-of-fit $= [\Sigma w(F_o^2 - F_c^2)^2 / (n_{obs} - n_{param})]^{1/2}$.
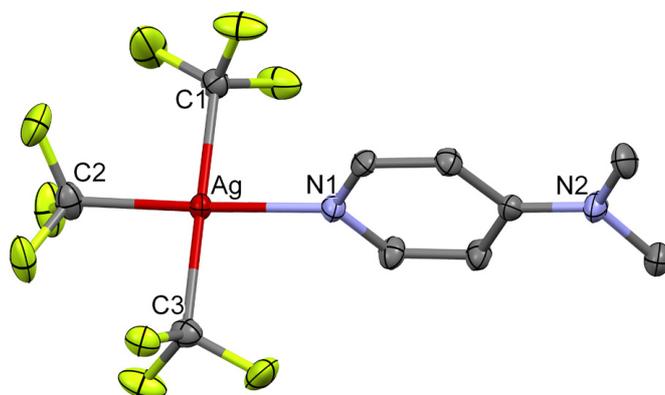
Table S11. Interatomic distances [pm] and angles [°] for $(CF_3)_3Ag(dmap)$ as found in crystals of **3** with atom labelling as indicated above.

|			
Ag–C(1)	209.6(3)	C(1)–Ag–C(2)	90.43(14)
Ag–C(2)	205.2(4)	C(1)–Ag–C(3)	176.25(14)
Ag–C(3)	208.9(4)	C(1)–Ag–N(1)	88.73(12)
Ag–N(1)	209.8(3)	C(2)–Ag–C(3)	89.22(15)
		C(2)–Ag–N(1)	176.07(13)
av. C(1)–F	134.4(4)	C(3)–Ag–N(1)	91.87(13)
av. C(2)–F	133.8(4)		
av. C(3)–F	135.6(4)	av. Ag–C(1)–F	114.1(2)
		av. Ag–C(2)–F	112.8(2)
		av. Ag–C(3)–F	113.9(2)
		av. F–C(1)–F	104.5(3)
		av. F–C(2)–F	105.9(3)
		av. F–C(3)–F	104.7(3)

Table S12. Crystal data and structure refinement for compound $(CF_3)_3Ag(PPh_3)\cdot\frac{1}{4}CH_2Cl_2$ (**4**$\cdot\frac{1}{4}CH_2Cl_2$)

formula	$C_{21}H_{15}AgF_9P\cdot$ $\frac{1}{4}(CH_2Cl_2)$
M_t [g mol^{-1}]	598.40
T [K]	100(2)
λ [pm]	71.073
crystal system	monoclinic
space group	$P2_1/n$
a [pm]	1157.973(19)
b [pm]	958.956(15)
c [pm]	3955.58(6)
β [°]	93.1699(14)
V [nm^3]	4.38573(12)
Z	8
ρ [g cm^{-3}]	1.813
μ [mm^{-1}]	1.136
$F(000)$	2356
2θ range [°]	5.6–56.7
no. of reflns colltd	43926
no. of unique reflns	9756
R_{int}	0.0336
R indices [$I > 2\sigma(I)$]^a	
R_1	0.0276
wR_2	0.0565
R indices (all data)	
R_1	0.0348
wR_2	0.0597
goodness-of-fit^b on F^2	1.052
CCDC no.	2226909

^{a} $R_1 = \Sigma(|F_o| - |F_c|) / \Sigma|F_o|$; $wR_2 = [\Sigma w(F_o^2 - F_c^2)^2 / \Sigma w(F_o^2)^2]^{1/2}$.
^{b} Goodness-of-fit $= [\Sigma w(F_o^2 - F_c^2)^2 / (n_{obs} - n_{param})]^{1/2}$.
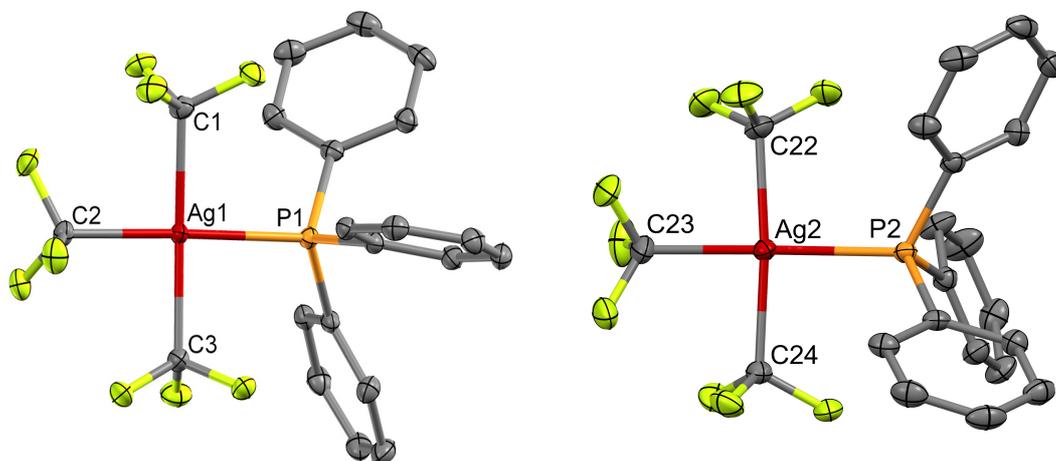
Table S13. Relevant interatomic distances [pm] and angles [°] averaged for the two independent molecules of $(CF_3)_3Ag(PPh_3)$ found in crystals of **4**.

Ag–P	242.38(6)	*trans*-C–Ag–C'	172.39(9)
(P)Ag–C	211.2(2)	*cis*-C–Ag–C'	88.16(9)
(C)Ag–C	211.6(2)	*trans*-C–Ag–P	177.50(7)
C–F	135.3(3)	*cis*-C–Ag–P	91.96(7)
P–C	181.5(2)		
		Ag–C–F	113.41(16)
		Ag–P–C	112.12(7)
		F–C–F	105.25(19)

Table S14. Crystal data and structure refinement for compound $(CF_3)_3Ag(AsPh_3)\cdot Me_2CO$ (**5**$\cdot$Me$_2$CO)

formula	$C_{24}H_{21}AgAsF_9O$
M_t [g mol^{-1}]	679.20
T [K]	100(2)
λ [pm]	71.073
crystal system	monoclinic
space group	$P2_1/n$
a [pm]	1495.873(16)
b [pm]	933.507(10)
c [pm]	1831.459(18)
β [°]	91.3241(10)
V [nm^3]	2.55678(5)
Z	4
ρ [g cm^{-3}]	1.764
μ [mm^{-1}]	2.154
$F(000)$	1336
2θ range [°]	5.6–56.8
no. of reflns colltd	47400
no. of unique reflns	5899
R_{int}	0.0307
R indices $[I > 2\sigma(I)]^a$	
R_1	0.0201
wR_2	0.0475
R indices (all data)	
R_1	0.0238
wR_2	0.0459
goodness-of-fit^b on F^2	1.025
CCDC no.	2226910

[a] $R_1 = \Sigma(|F_o| - |F_c|) / \Sigma|F_o|$; $wR_2 = [\Sigma w(F_o^2 - F_c^2)^2 / \Sigma w(F_o^2)^2]^{1/2}$.
[b] Goodness-of-fit $= [\Sigma w(F_o^2 - F_c^2)^2 / (n_{obs} - n_{param})]^{1/2}$.
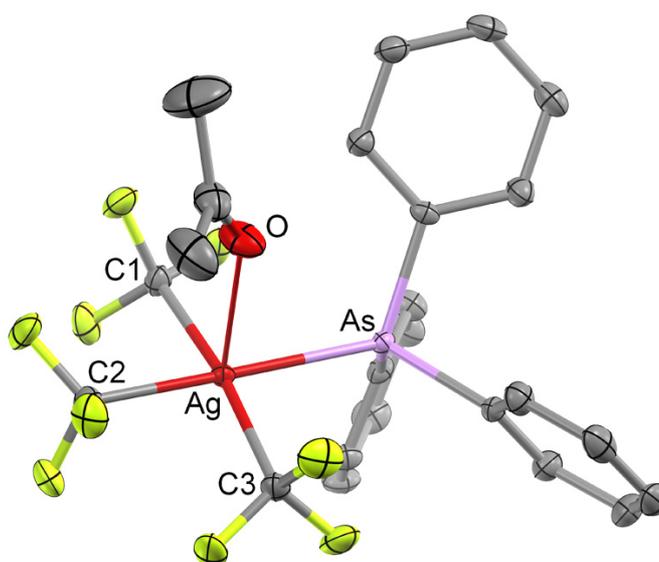
Table S15. Interatomic distances [pm] and angles [°] for $(CF_3)_3Ag(AsPh_3) \cdot Me_2CO$ as found in crystals of **5**·Me_2CO with atom labelling as indicated above.[a]

|			
Ag–C(1)	211.56(17)	C(1)–Ag–C(2)	88.10(7)
Ag–C(2)	210.14(17)	C(1)–Ag–C(3)	170.64(7)
Ag–C(3)	210.95(17)	C(1)–Ag–As	90.88(5)
Ag–As	251.365(19)	C(2)–Ag–C(3)	88.60(7)
Ag–O	265.30(14)	C(2)–Ag–As	178.98(5)
av. C(1)–F	135.7(2)	C(3)–Ag–As	92.40(5)
av. C(2)–F	134.0(2)		
av. C(3)–F	135.1(2)	av. Ag–C(1)–F	113.86(12)
av. As–C	193.22(16)	av. Ag–C(2)–F	112.56(12)
		av. Ag–C(3)–F	113.77(12)
Ag–O–C(22)	148.1(1)		
		av. F–C(1)–F	104.73(14)
		av. F–C(2)–F	106.21(15)
		av. F–C(3)–F	104.84(14)
		av. Ag–As–C	114.73(5)
		av. C–As–C'	103.76(7)

[a] The Ag–O line deviates just 3.8(1)° from the normal to the best basal plane.

4. Computational Details

Quantum mechanical calculations were performed with the Gaussian09 package[S7] at the DFT/M06 level of theory with an ultrafine grid option[S8] and supplemented with Grimme's dispersion correction D3.[S9] All elements (H, C, N, O, F, P, As, and Ag) have been described using a Ahlrichs' def2-TZVPD basis set,[S10] a Triple-Zeta-Valence basis set including Polarization and Diffuse basis functions, as obtained from the Basis Set Exchange webpage.[S11,S12] The geometries of the different complexes have been optimized in the gas phase with no symmetry restrictions. The optimized $(CF_3)_3Ag(L)$ molecules were found to exhibit square-planar geometry (Fig. S8). The interaction of these metal complexes with an additional donor molecule L′ was found to be stabilizing in all cases (Table S16); the optimized geometries of the resulting $(CF_3)_3Ag(L) \cdot L'$ molecules are shown in Fig. S9 (L′ = MeCN) and Fig. S10 (L′ = Me_2CO). Frequency calculations were performed in all the collected stationary points in order to check their nature of minima. Atomic coordinates for all the optimized structures are included as a separate *.xyz* file.
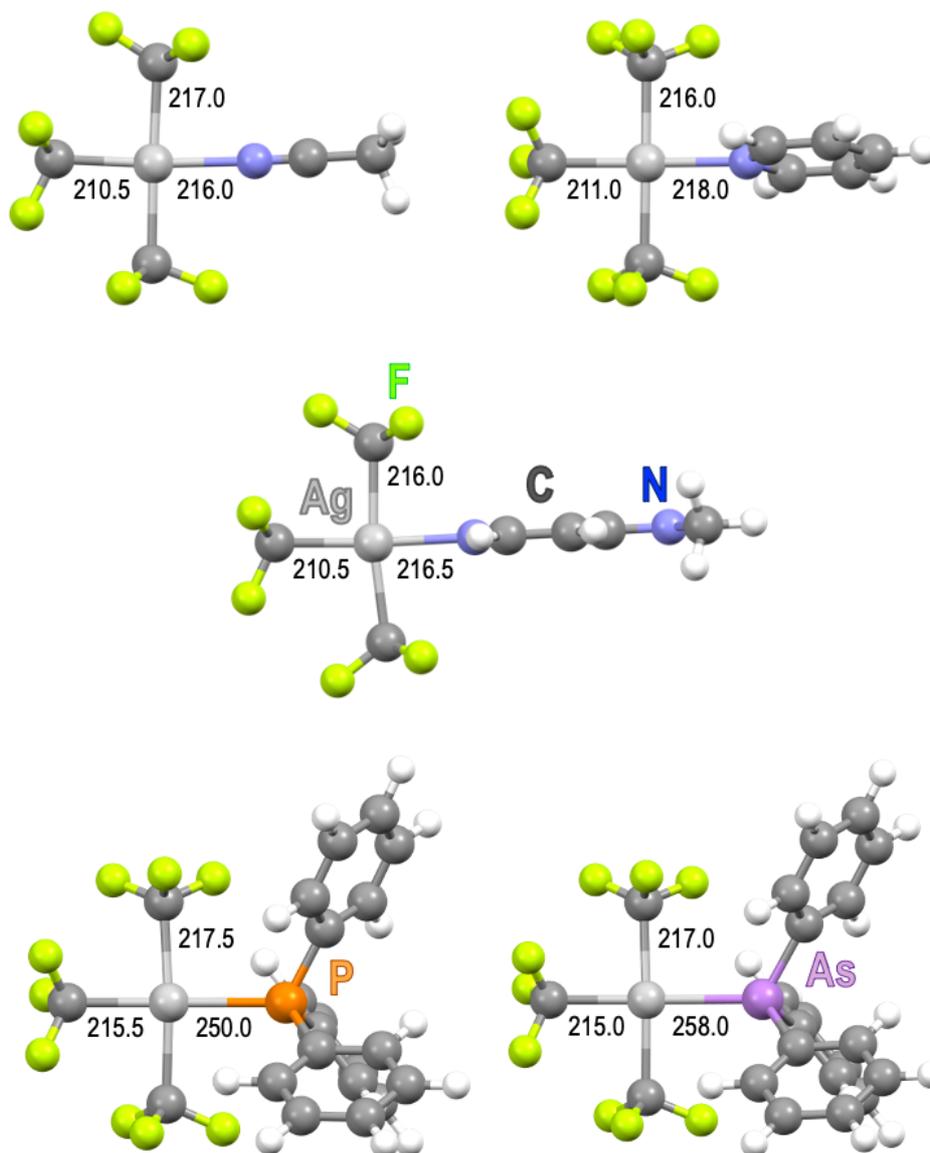
Fig. S8. Optimized structures of the $(CF_3)_3Ag(L)$ molecules **1**–**5** with relevant calculated interatomic distances [pm] indicated. Slightly elongated Ag–E distances in comparison with the corresponding experimental values are consistently obtained.
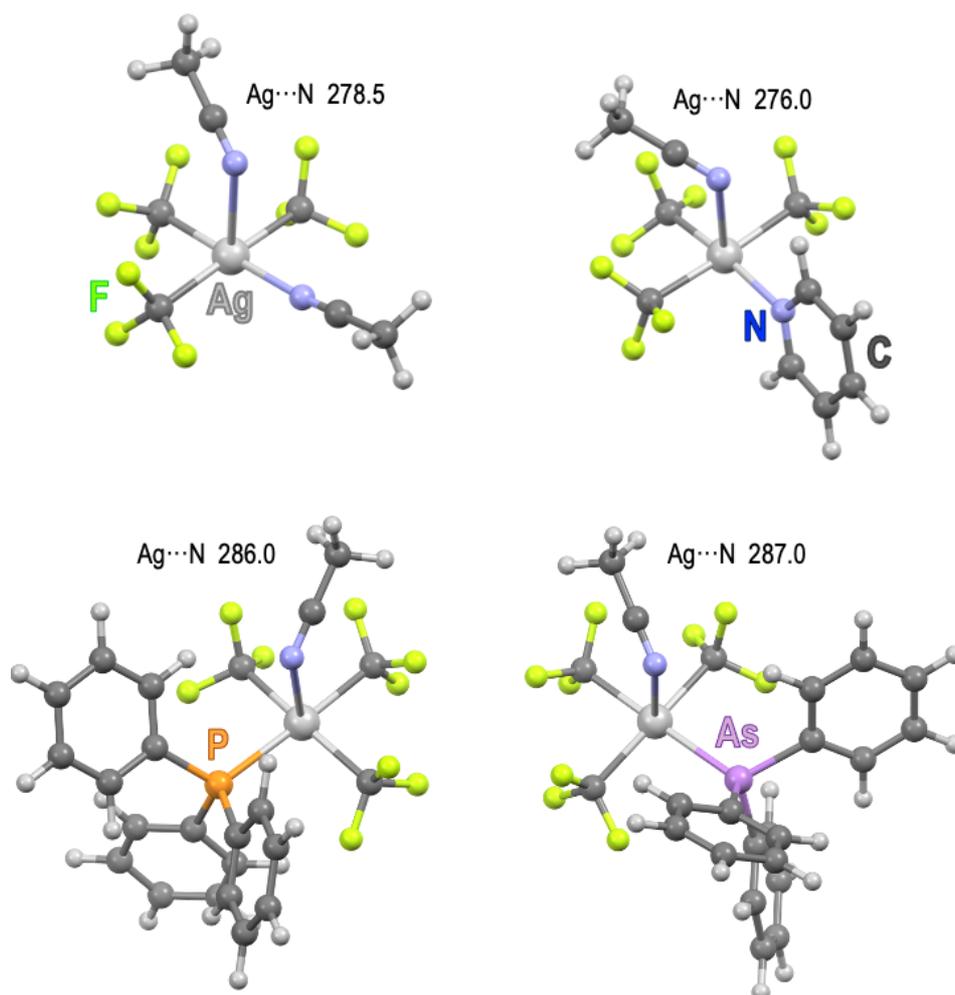
Fig. S9. Optimized structures of the $(CF_3)_3Ag(L) \cdot NCMe$ molecules. The additional interaction is freely located at the apical site and is stabilizing in all cases with the calculated $Ag \cdots N$ distances [pm] indicated. Slightly elongated Ag–E distances in comparison with the corresponding experimental values are consistently obtained.
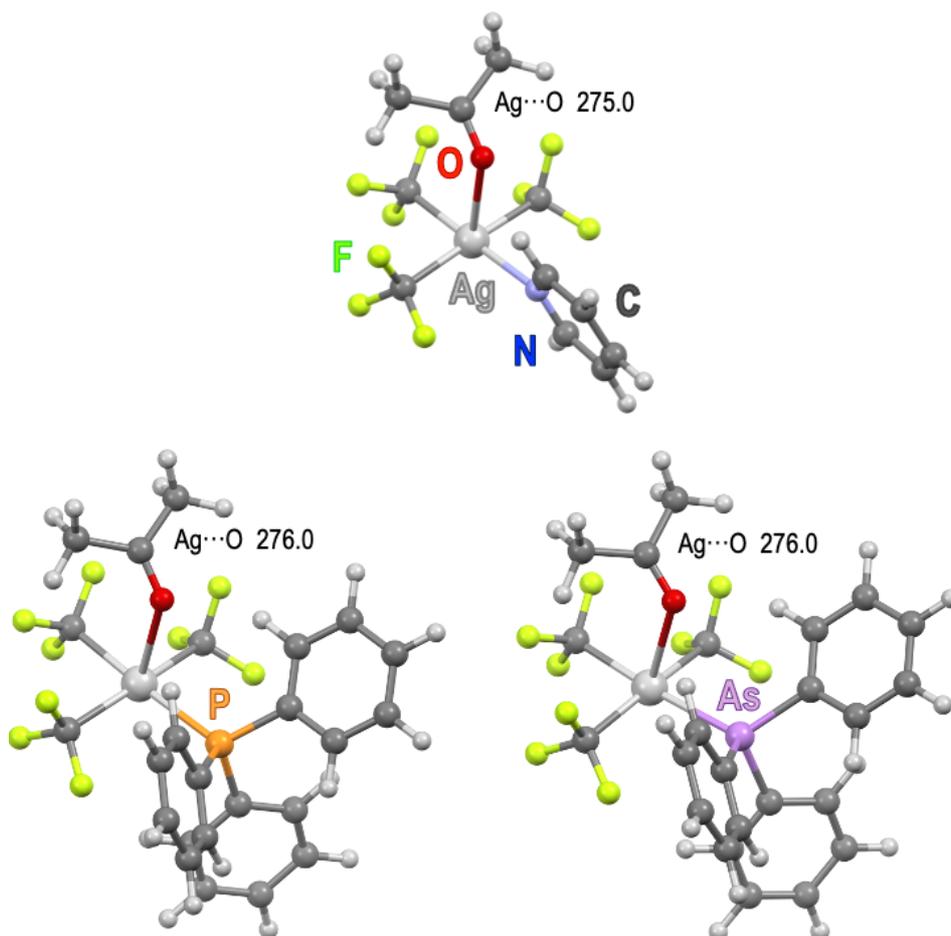
Fig. S10. Optimized structures of the $(CF_3)_3Ag(L)\cdot OCMe_2$ molecules. The additional interaction is freely located at the apical site and is stabilizing in all cases with the calculated Ag⋯O distances [pm] indicated. Slightly elongated Ag–E distances in comparison with the corresponding experimental values are consistently obtained.

Table S16. Energy involved in the non-assisted interaction of the given neutral complex $(CF_3)_3Ag(L)$ with an additional L′ ligand in the gas phase.[a]

Complex	ΔH [kcal mol^{-1}]	
	L′ = MeCN	L′ = Me$_2$CO
$(CF_3)_3Ag(NCMe)$	−8.5	—
$(CF_3)_3Ag(py)$	−11.4	−10.8
$(CF_3)_3Ag(PPh_3)$	−10.6	−11.4
$(CF_3)_3Ag(AsPh_3)$	−11.1	−12.0

[a] Values calculated at the DFT/M06-GD3/def2-TZVPD level of theory; the optimized geometries of the corresponding $(CF_3)_3Ag(L)\cdot L′$ molecules are shown in Fig. S9 (L′ = MeCN) and Fig. S10 (L′ = Me$_2$CO).

6. References

S1   D. Joven-Sancho, M. Baya, L. R. Falvello, A. Martín, J. Orduna and B. Menjón, *Chem. Eur. J.*, 2021, **27**, 12796.

S2   D. Naumann, W. Tyrra, F. Trinius, W. Wessel and T. Roy, *J. Fluorine Chem.*, 2000, **101**, 131.

S3   R. Eujen, B. Hoge and D. J. Brauer, *Inorg. Chem.*, 1997, **36**, 1464.

S4   *CrysAlis Pro* 1.171.39.44a, Rigaku Oxford Diffraction 2018.

S5   *SADABS*, Bruker AXS Inc., Madison, Wisconsin, USA, 2016.

S6   SHELXL Version 2014/8: G. M. Sheldrick, *Acta Crystallogr. Sect. C* 2015, **71**, 3.

S7   M. J. Frisch, G. W. Trucks, H. B. Schlegel, G. E. Scuseria, M. A. Robb, J. R. Cheeseman, G. Scalmani, V. Barone, B. Mennucci, G. A. Petersson, H. Nakatsuji, M. Caricato, X. Li, H. P. Hratchian, A. F. Izmaylov, J. Bloino, G. Zheng, J. L. Sonnenberg, M. Hada, M. Ehara, K. Toyota, R. Fukuda, J. Hasegawa, M. Ishida, T. Nakajima, Y. Honda, O. Kitao, H. Nakai, T. Vreven, J. A. Montgomery, Jr., J. E. Peralta, F. Ogliaro, M. Bearpark, J. J. Heyd, E. Brothers, K. N. Kudin, V. N. Staroverov, T. Keith, R. Kobayashi, J. Normand, K. Raghavachari, A. Rendell, J. C. Burant, S. S. Iyengar, J. Tomasi, M. Cossi, N. Rega, J. M. Millam, M. Klene, J. E. Knox, J. B. Cross, V. Bakken, C. Adamo, J. Jaramillo, R. Gomperts, R. E. Stratmann, O. Yazyev, A. J. Austin, R. Cammi, C. Pomelli, J. W. Ochterski, R. L. Martin, K. Morokuma, V. G. Zakrzewski, G. A. Voth, P. Salvador, J. J. Dannenberg, S. Dapprich, A. D. Daniels, O. Farkas, J. B. Foresman, J. V. Ortiz, J. Cioslowski and D. J. Fox; *Gaussian 09, Revision D.01* Gaussian, Inc., Wallingford CT, 2013.

S8   Y. Zhao and D. G. Truhlar, *Theor. Chem. Acc.*, 2008, **120**, 215.

S9   S. Grimme, J. Antony, S. Ehrlich and H. Krieg, *J. Chem. Phys.*, 2010, **132**, 154104.

S10   (a) D. Rappoport and F. Furche, *J. Chem. Phys*., 2010, **133**, 134105; (b) F. Weigend and R. Ahlrichs, *Phys. Chem. Chem. Phys*., 2005, **7**, 3297; (c) K. A. Peterson, D. Figgen, E. Goll, H. Stoll and M. Dolg, *J. Chem. Phys*., 2003, **119**, 11113; (d) D. Andrae, U. Häußermann, M. Dolg, H. Stoll and H. Preuß, *Theor. Chim. Acta*, 1990, **77**, 123.

S11   Basis Set Library obtained from: https://www.basissetexchange.org/

S12   (a) D. Feller, *J. Comput. Chem.*, 1996, **17**, 1571; (b) K. L. Schuchardt, B. T. Didier, T. Elsethagen, L. Sun, V. Gurumoorthi, J. Chase, J. Li and T. L. Windus, *J. Chem. Inf. Model.*, 2007, **47**, 1045.